

# Extending the Mossakovskii method to contacts supporting a moment

Matthew R. Moore<sup>a,\*</sup>, David. A. Hills<sup>b</sup>

<sup>a</sup>*Mathematical Institute, Radcliffe Observatory Quarter, St. Giles, Oxford, OX2 6GG, UK.*

<sup>b</sup>*Department of Engineering Science, Parks Road, Oxford OX1 3PJ, UK.*

---

## Abstract

In this article, we extend the Mossakovskii approach to half-plane contacts supporting a moment. Since the method relies on approximating the punch geometry by a series of flat punches, we choose the load path in  $(P, M)$ -space that fixes the body tilt, which allows us to reduce the standard Cauchy singular integral formulation to a non-symmetric Abel integral equation. We use the formulation to derive simple expressions for the applied normal force and necessary applied moment as functions of the contact extent and indenter tilt, while also deriving the coefficients of the square-root terms in the contact pressure expansion at the edges of the contact. These results are analysed in detail for two specific examples: the tilted wedge and the tilted flat-and-rounded punch. We conclude by briefly discussing the equivalent tangential problem when an applied shear force and differential bulk tensions are present.

*Keywords:* Half-plane theory, B. Contact mechanics, C. Asymptotic analysis

---

## 1. Introduction

Half-plane theory is a well-established model for considerations of contact problems relevant to large-scale industrial applications. The contacting bodies are assumed to be sufficiently large that local to the contact, a half-plane idealisation derived from the Flamant solution for the stress field due to a line force at the apex of a wedge is a reasonable approximation [4, 5]. In the limit in which the contacting bodies are elastically similar, the problems for the normal and tangential displacement gradients — gradients to circumvent the problem of the unknown rigid-body terms in the formulation — decouple. For the purposes of this analysis, we shall concentrate on the normal displacement gradients primarily, although much of what we discuss will be applicable to the tangential problem as well, and we return to this topic later.

Consider the formulation in figure 1 where the  $(x, y)$ -plane has been chosen so that the origin is at the minimum of the upper body, which has profile  $y = g(x)$ . We define the relative normal displacement of the contacting bodies as  $v = v_1(x) - v_2(x)$ , where a subscript 1 denotes the upper body and a subscript 2 denotes the lower body. Then, for elastically-similar bodies, the relative normal displacement gradient is related to the contact

---

\*Corresponding author: [moorem@maths.ox.ac.uk](mailto:moorem@maths.ox.ac.uk).

17 pressure  $p(x)$  by the following integral equation

$$\frac{dv}{dx} = \frac{\kappa + 1}{2\mu\pi} \int_{-b}^a \frac{p(s)}{s - x} ds, \quad (1)$$

18 where  $(-b, a)$  is the contact patch,  $\kappa$  is Kolosov's constant and  $\mu$  is the modulus of rigidity.  
19 When  $-b < x < a$ , (1) is interpreted in the Cauchy principal value sense, otherwise it is  
20 regular. Within the contact set, we know that

$$v'(x) + g'(x) = 0 \quad \text{for} \quad -b < x < a, \quad (2)$$

21 where a prime indicates differentiation with respect to argument, so that, for a given ge-  
22 ometry, one can invert (1) to find the contact pressure following the methodology of, for  
23 example, [10]. In particular, since in an incomplete contact the contact pressure is bounded  
24 at the ends of the contact patch, a consistency condition relating  $a$  and  $b$  must be satisfied  
25 for a solution to exist, namely

$$0 = \int_{-b}^a \frac{v'(s)}{\sqrt{(a-s)(s+b)}} ds. \quad (3)$$

26 Over recent years, there has been much consideration of (1) in partial slip problems, see  
27 for example [6, 7, 13, 16, 18] and references therein. Although there are notable exceptions  
28 such as [3, 8], the singular integral formulation can prove analytically and numerically tricky  
29 to handle. An alternative formulation of the problem devised by Mossakovskii [17] and  
30 extended by [11, 14, 20] utilises the known contact pressure induced by a flat punch to  
31 approximate the upper body by an infinite series of flat punches, which reduces the singular  
32 integral to an Abel integral equation, which can be inverted. However, in each of these  
33 studies, the consideration has been for symmetric problems (i.e.  $b = a$ ), which precludes the  
34 presence of a moment. In many industrial applications, for example in oil wellheads or the  
35 dovetail joint of a turbine blade, the presence of an applied moment is inevitable.

36 In this study, we adapt the Mossakovskii method to problems with an applied moment.  
37 In §2, we shall formulate the problem and derive the corresponding non-symmetric Abel  
38 integral formulation. We shall use this formulation to derive general results for the applied  
39 normal force and applied moment, as well as the behaviour of the contact pressure at the ends  
40 of the contact patch in §3. We move on to discuss the solution for two specific examples in  
41 §4, the tilted wedge and the tilted flat-and-rounded punch. In §5, we return to the tangential  
42 problem and consider applications of the method there, before concluding with a summary  
43 and discussion in §6.

## 44 2. Problem formulation

45 We consider the problem depicted in figure 1, in which a body with profile  $y = g(x)$  is  
46 brought into contact with an elastically-similar half-plane under an applied normal force,  $P$ .  
47 We shall assume at the outset that the geometry is known and fixed as  $P$  varies, so that  
48 there is no relative rotation of the body as we change  $P$ . Nevertheless, for non-symmetric  
49 geometries about the origin, an applied moment,  $M$ , is necessary to maintain the contact  
50 in this orientation. The geometrical constraint is necessary for the Mossakovskii method to

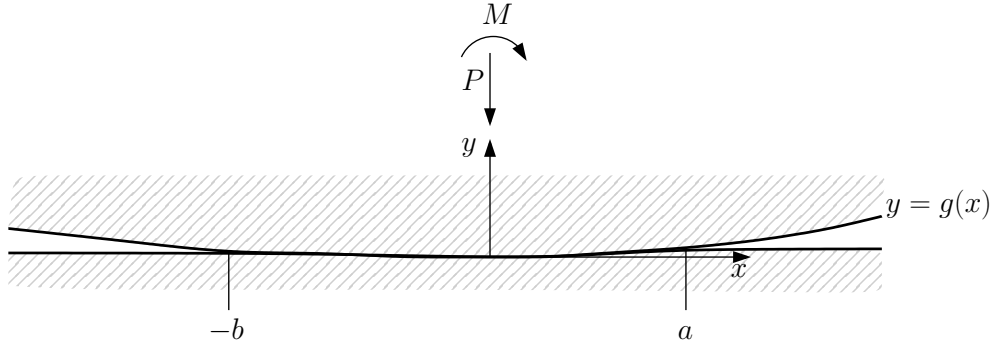


Figure 1: A large, almost flat body  $y = g(x)$  is pressed into an elastically-similar half-space with an applied normal force,  $P$ , and an applied moment,  $M$ . The contact patch extends over  $(-b, a)$ .

51 apply, else in general we run into issues with the minimum of the punch changing as  $M, P$   
 52 vary and the punch rotates. Hence, we restrict ourselves to a particular load path in  $(P, M)$   
 53 space that fixes the geometry, and as is well-known, the final results for, for example, the  
 54 contact pressure, are the same as had we taken a different load path. Thus our assumption  
 55 is not overly restrictive. We shall discuss this further in §3.2.

56 We know that the contact pressure in the contact patch  $-b < x < a$  is related to the  
 57 relative normal displacement gradient by (1) and that to maintain vertical equilibrium, we  
 58 must have

$$P = \int_{-b}^a p(s) ds. \quad (4)$$

59 If we take  $P$  and the indenter geometry  $g(x)$  as known, then we can view (3) and (4) as a  
 60 pair of equations for  $a, b$ . Moreover, these equations are uncoupled: in particular, we shall  
 61 view (3) as an equation that gives  $b$  as a function of  $a$  for a specific geometry. Once this has  
 62 been solved, then (4) gives  $a$  as a function of  $P$ . For the rest of this analysis, we shall assume  
 63 that  $b(a)$  is known and that as  $P$  increases, both  $a$  and  $b(a)$  increase (which is reasonable  
 64 provided the body is convex).

65 Given these results, we can adapt the methodology of [11] to contacts supporting a  
 66 moment by considering the non-symmetric flat punch in figure 2. It is straightforward to  
 67 show that substituting the pressure distribution  $m(x, a)$ , where

$$m(x, a) = \begin{cases} \frac{1}{\sqrt{(a-x)(x+b(a))}} & \text{for } -b(a) < x < a, \\ 0 & \text{otherwise} \end{cases}, \quad (5)$$

68 corresponds to that of a flat punch by substituting into (1), which gives

$$\frac{dv}{dx} = \frac{\kappa + 1}{2\mu\pi} h(x, a) = \frac{\kappa + 1}{2\mu\pi} \begin{cases} 0 & \text{for } -b(a) < x < a, \\ \frac{-\text{sgn}(x)\pi}{\sqrt{(x-a)(x+b)}} & \text{otherwise} \end{cases}. \quad (6)$$

69 The Mossakovskii idea is then to replace the indenter by an infinite superposition of flat  
 70 punches, so that

$$p(x, a) = \int_0^a F(s) m(x, s) ds, \quad (7)$$

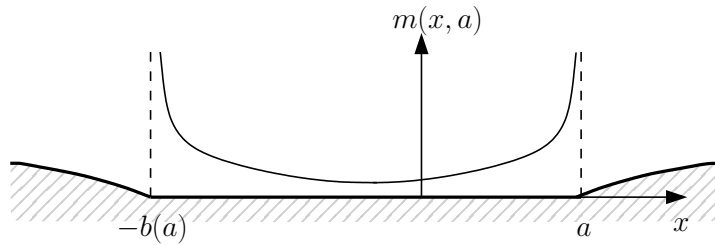


Figure 2: The complete contact of a flat punch extending over  $(-b(a), a)$  and the associated contact pressure  $m(x, a)$  given by (5).

71 where the aim is to relate the unknown function  $F(s)$  to the indenter geometry. By the  
 72 previous analysis, we see that

$$\frac{dv}{dx} = \frac{\kappa + 1}{2\mu\pi} \int_0^a F(s)h(x, s) ds \quad (8)$$

73 for all  $-b(a) < x < a$ . Hence, by (2), we must have

$$\frac{2\mu g'(x)}{\kappa + 1} = \int_0^x \frac{F(s)}{\sqrt{(x-s)(x+b(s))}} ds \text{ for } 0 < x < a, \quad (9)$$

74 and we obtain our solution provided that  $b(a)$  has been found from (3). Note that, without  
 75 loss of generality, we could equivalently solve for  $F(s)$  on  $(-b(a), 0)$ . The integral equation  
 76 (9) is a non-symmetric Abel integral equation for  $F(s)$ , which is, unfortunately, not readily  
 77 analytically inverted in general, unlike in the symmetric problem, [11]. It is however relatively  
 78 straightforward to deal with numerically, particularly as we have removed the singularity  
 79 associated with the standard inversion procedure, [10]. We discuss such a procedure for a  
 80 specific example in §4.2 and Appendix B.

81 Once we have found  $F(s)$ , the contact pressure is then given by

$$p(x, a) = \begin{cases} \int_x^a \frac{F(s)}{\sqrt{(s-x)(x+b(s))}} ds & \text{for } 0 < x < a, \\ \int_{b^{-1}(-x)}^a \frac{F(s)}{\sqrt{(s-x)(x+b(s))}} ds & \text{for } -b(a) < x < 0, \\ 0 & \text{otherwise,} \end{cases} \quad (10)$$

82 where  $b^{-1}(\cdot)$  denotes the inverse of  $b(\cdot)$ . To elucidate how the lower limit of the second integral  
 83 has been obtained, we recall that since we have assumed  $b(\cdot)$  is an increasing function, then  
 84 for all  $-b(a) < x < 0$ , there exists a unique  $s \in (0, a)$  such that  $b(s) = -x$ . Then, for  
 85  $s < b^{-1}(-x)$ , by (5) the contribution of  $m(x, s)$  in the integrand is necessarily zero.

### 86 3. General results

#### 87 3.1. Applied normal force

88 We recall the vertical equilibrium condition (4). Upon substituting (7) into (4), we have

$$P = \int_0^a F(s) \int_{-b(a)}^a m(x, s) dx ds = \int_0^a F(s) \int_{-b(s)}^s \frac{1}{\sqrt{(s-x)(x+b(s))}} dx ds. \quad (11)$$

89 Thus, changing variables in the inner integral by setting

$$x = \frac{s - b(s)}{2} + \frac{(s + b(s))}{2}X \quad (12)$$

90 yields

$$P = \pi \int_0^a F(s) ds \text{ or, equivalently, } F(a) = \frac{1}{\pi} \frac{dP}{da}, \quad (13)$$

91 as in the symmetric case, [11]. Thus, we can replace the unknown function  $F(\cdot)$  by  $\pi^{-1}P'(\cdot)$   
 92 everywhere it appears in the analysis, provided that the initial condition  $P(0) = 0$  is applied  
 93 where necessary (i.e., there is no contact unless a normal force is supplied). We do so  
 94 henceforth, and in particular, the Abel equation (9) becomes

$$\frac{2\mu\pi g'(x)}{\kappa + 1} = \int_0^x \frac{P'(s)}{\sqrt{(x-s)(x+b(s))}} ds \text{ for } 0 < x < a, \quad (14)$$

95 subject to  $P(0) = 0$ , where a prime denotes differentiation. We note that the inversion of  
 96 (14) will give  $P(s)$  for  $0 < s < a$ .

### 97 3.2. Applied moment

98 To find the applied moment,  $M$ , necessary to sustain the contact, we must have

$$M = \int_{-b(a)}^a sp(s) ds. \quad (15)$$

99 After performing a similar analysis, we find that

$$M = \frac{1}{2} \int_0^a (s - b(s))P'(s) ds = \frac{1}{2} \left[ P(a)(a - b(a)) - \int_0^a P(s)(1 - b'(s)) ds \right], \quad (16)$$

100 where we have integrated by parts to achieve the final equality.

101 Hence, (14) and (16) give  $P$  and  $M$  as functions of the indenter geometry  $g(x)$ . As we  
 102 alluded to at the start of §2, the methodology has relied on the geometry being maintained as  
 103  $P$  varies, so that we have chosen the particular load path in  $(P, M)$  space where  $M$  is given  
 104 by (16). While this is a constraint necessary for the approach to work, it is not necessarily  
 105 over-restrictive, as the results are load-path independent.

106 Hence, an algorithm for using the method for a general punch profile is as follows. Suppose  
 107 we are given a symmetric indenter  $y = h(x)$  that we tilt by an angle of  $\alpha$  to the horizontal. If  
 108 we denote the tilted indenter shape by  $y = g(x; \alpha)$  (the semicolon indicating that  $\alpha$  is acting  
 109 as a parameter, not a variable), then (14) and (16) can be used to find the  $P$  and  $M$  necessary  
 110 to sustain a contact over  $(-b(a), a)$  with tilt  $\alpha$ . We can then repeat the process varying the  
 111 value of  $\alpha$ , which populates the space  $P(a, \alpha)$  and  $M(a, \alpha)$ . One can then consider a general  
 112 loading curve in  $(P, M)$ -space and find the resulting values of  $\alpha$ . We will illustrate this in the  
 113 simple case of a tilted wedge in §4.1. Naturally, there may also be applications for problems  
 114 in which the constancy of the tilted geometry is required, and this methodology thus gives  
 115 the necessary applied moment (16) to provide this as  $P$  changes.

116 *3.3. Application to asymptotic approaches*

117 Finally, we note that there has been a lot of recent work in the field of asymptotic methods  
 118 for partial slip problems in which the stress-fields local to the edges of contact are crucial  
 119 in understanding the onset of fretting fatigue in large industrial machinery, [1, 9, 12]. The  
 120 idea is to consider the problem locally where the geometry may be simpler — for example,  
 121 a flat-and-rounded punch may be taken as Hertzian near the edges of the contact — and  
 122 use knowledge of the local form of the contact pressure (and shear traction  $q(x)$ ) to set up a  
 123 problem with suitably-chosen far-field bulk tensions and/or shear forces to obtain slip-zones  
 124 of the same size. The simpler geometry is then easier to study in laboratory prototypes and  
 125 numerical studies. Such methods may also be of use in problems where the slip zones have  
 126 opposite signs and hence, the Ciavarella-Jäger theorem no longer applies, [2].

127 In these cases, the punch geometry will be known (perhaps from finite element solutions  
 128 or otherwise) for general input conditions  $P$ ,  $M$  and applied shear forces and bulk tensions  
 129 (usually denoted  $Q$  and  $\sigma$ ). Given the geometry, one can use the Mossakovskii method to  
 130 extract quickly the local coefficient of the contact pressure (and shear tractions, see §5) at  
 131 the contact edges,  $K_{n,a}$  and  $K_{n,b}$ , without the difficulties associated with extracting them  
 132 numerically. It is straightforward to perform an asymptotic expansion of the integral (7) as  
 133  $x$  approaches the edges of the contact to deduce

$$p = \frac{2}{\pi} \frac{P'(a)}{\sqrt{a+b(a)}} \sqrt{a-x} + o(\sqrt{a-x}) \text{ as } x \rightarrow a^-, \text{ so that } K_{n,a} = \frac{2}{\pi} \frac{P'(a)}{\sqrt{a+b(a)}}, \quad (17)$$

134 while

$$p = \frac{2}{\pi} \frac{P'(a)}{b'(a)\sqrt{a+b(a)}} \sqrt{b(a)+x} + o(\sqrt{b(a)+x}) \text{ as } x \rightarrow -b(a)^+, \text{ so that } K_{n,b} = \frac{2}{\pi} \frac{P'(a)}{b'(a)\sqrt{a+b(a)}}, \quad (18)$$

135 where we have relegated the details to Appendix A. In particular, we note that  $K_{n,b} =$   
 136  $K_{n,a}/b'(a)$ .

137 **4. Application to specific geometries**

138 *4.1. The tilted wedge*

139 Consider a large wedge of half-angle  $\pi/2 - \phi$ , where  $0 < \phi \ll 1$ , that is tilted at an angle  
 140  $\alpha < \phi$  measured clockwise from the unrotated state, see figure 3. Since we are assuming that  
 141 the wedge half-angle is large enough that we can reasonably use a half-space approximation  
 142 for the contact, the wedge profile is approximated by

$$g(x) = \begin{cases} \Delta - (\phi + \alpha)x & \text{for } x < 0 \\ \Delta + (\phi - \alpha)x & \text{for } x > 0 \end{cases}, \quad (19)$$

143 where  $\Delta$  is a rigid-body translation.

144 By the geometry of the problem, we expect there to be a similarity solution, so that  
 145  $b = \gamma a$  for some  $\gamma \geq 0$ . Upon evaluating (3), we find

$$\gamma = \left(1 - \sin\left(\frac{\pi\alpha}{2\phi}\right)\right) \left(1 + \sin\left(\frac{\pi\alpha}{2\phi}\right)\right)^{-1}, \quad (20)$$

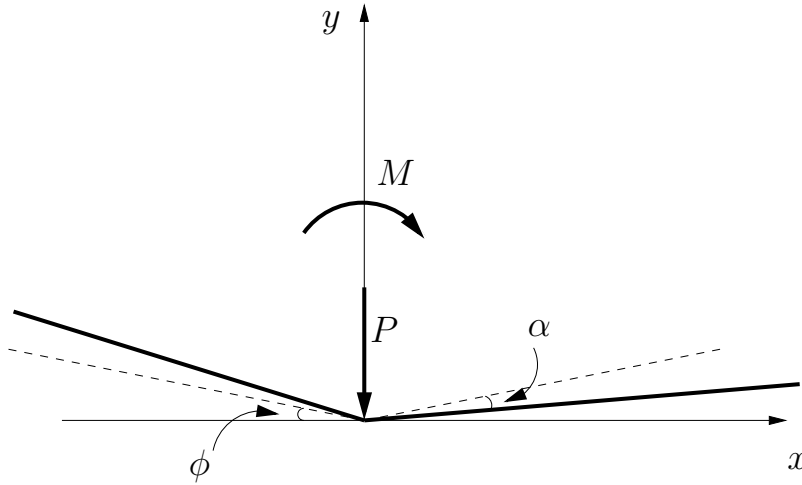


Figure 3: A large, almost flat tilted wedge of half-angle  $\phi$  and tilt angle  $\alpha$ . The normal force  $P$  is applied through the wedge apex (i.e. at the coordinate origin), along with a moment  $M$  about the  $y$ -axis.

146 as in [19].

147 Similarly, seeking a solution of the form  $P(a) = P_0 a$ , we can invert (14) to find that

$$P_0 = \frac{4\mu\phi}{\kappa + 1} \sqrt{\gamma}, \quad (21)$$

148 which we note is again consistent with [19]. Note that the corresponding contact pressure is  
149 given by

$$p(x) = \frac{-4\mu\phi}{\pi(\kappa + 1)} \log \left| \frac{\sqrt{1/\gamma} - \sqrt{(a-x)/(x+\gamma a)}}{\sqrt{1/\gamma} + \sqrt{(a-x)/(x+\gamma a)}} \right|. \quad (22)$$

150 Finally, we can utilise (16) to show that

$$M(a) = \frac{P_0}{4} (1 - \gamma) a^2, \quad (23)$$

151 is the moment necessary to maintain such a contact. Noting that there is a sign error in  
152 equation (27) of [19], one can in fact also show that (23) is consistent with their result once  
153 the corrected algebra is performed.

154 We can now manipulate (21), (23) to find the dependence of  $a$  and  $\alpha$  on  $P$ ,  $M$ . Hence if  
155  $P, M$  are given, we can find  $\alpha$  from

$$\frac{(\kappa + 1) P^2}{16\mu\phi M} = \frac{\sqrt{\gamma}}{1 - \gamma}, \quad (24)$$

156 which, utilising (20), yields

$$\alpha = \frac{2\phi}{\pi} \arcsin \left( \frac{8\mu\phi M}{\sqrt{64\mu^2\phi^2 M^2 + (\kappa + 1)^2 P^4}} \right), \quad (25)$$

157 where we have assumed  $\alpha > 0$  without loss of generality due to the symmetry of the indenter.  
158 Note that for fixed  $P$ , as  $M \rightarrow 0$ , we see that  $\alpha \rightarrow 0$  as expected.

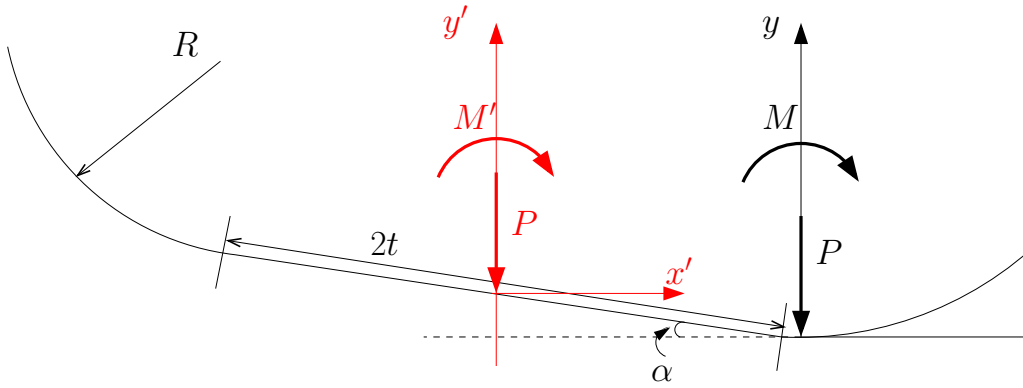


Figure 4: (Colour online.) A flat-and-rounded punch with flat section of size  $2t$ , rounded radius of curvature,  $R$ , and tilt angle  $\alpha$  to the horizontal. The coordinate axes  $(x', y')$  and  $(x, y)$ , and their respective associated applied normal forces and moments  $(P, M')$  and  $(P, M)$  are discussed in detail in the text.

159 In a similar manner,  $a$  is given as a function of  $P$  and  $M$  by

$$a = \frac{(\kappa + 1)^2 P^3}{4\mu\phi} \frac{1}{-8\mu\phi M + \sqrt{64\mu^2\phi^2 M^2 + (\kappa + 1)^2 P^4}}. \quad (26)$$

160 where the negative root has been discounted as that gives  $a < 0$ . We should note the limit  
 161 in which  $M = 0$  returns the expected relation between  $a$  and  $P$ , while the limit in which  
 162  $P \rightarrow 0$  and  $M$  is finite is singular in the sense that both the numerator and denominator  
 163 vanish simultaneously. Again, this is as expected, since the limit in which there is no applied  
 164 normal force but merely a moment makes no sense physically in this problem.

165 Hence for the wedge, we are able to invert the problem to one of finding  $a$  and  $\alpha$  when  
 166 given  $M$  and  $P$ . We are able to do this so simply for a wedge since the geometry is such  
 167 that as  $P$  and  $M$  change, the body rotates but the minimum remains fixed.

168 Finally, we note that  $K_{n,a}(a)$ , the coefficient of the square-root term in the pressure  
 169 expansion at the right-hand contact edge is given by (17) to be

$$K_{n,a} = \frac{8\mu\phi}{\pi(\kappa + 1)} \sqrt{\frac{\gamma}{a(1 + \gamma)}}. \quad (27)$$

170 and hence, at the left-hand contact point, by (18) we simply have

$$K_{n,b} = \frac{K_{n,a}}{\gamma}. \quad (28)$$

#### 171 4.2. The tilted flat-and-rounded punch

172 The flat-and-rounded punch is a geometry that is of great interest in industrial applica-  
 173 tions. Here we consider a punch whose flat length is  $2t$  that is rotated by a small angle  $\alpha$   
 174 clockwise. Since the Mossakovskii approach requires the approximation of the indenter by a  
 175 series of rectangular punches, we must consider the coordinate frame fixed with the minimum  
 176 of the punch. Thus, if in the frame fixed with the line of symmetry of the unrotated punch,



177 we have

$$y' = \begin{cases} \Delta - \alpha x' + \frac{(x' - t)^2}{2R} & \text{for } x' > t \\ \Delta - \alpha x' & \text{for } -t < x' < t, \\ \Delta - \alpha x' + \frac{(x' + t)^2}{2R} & \text{for } x' < -t \end{cases} \quad (29)$$

178 we make the change of variables

$$x' = R\alpha + t + x, \quad y' = \Delta - \frac{\alpha^2 R}{2} - \alpha t + y, \quad (30)$$

179 so that the punch is now given by  $y = g(x)$  where

$$g(x) = \begin{cases} -\frac{\alpha^2 R}{2} - \alpha x + \frac{(R\alpha + x)^2}{2R} & \text{for } x > -R\alpha \\ -\frac{\alpha^2 R}{2} - \alpha x & \text{for } -R\alpha - 2t < x < -R\alpha. \\ -\frac{\alpha^2 R}{2} - \alpha x + \frac{(R\alpha + 2t + x)^2}{2R} & \text{for } x < -R\alpha - 2t \end{cases} \quad (31)$$

180 The indenter is depicted in figure 4, with the original  $(x', y')$ -frame shown in red and the  
 181 shifted  $(x, y)$ -frame shown in black. We note that, in this analysis, the applied normal force  
 182 and applied moment  $(P, M)$  are measured with respect to the  $(x, y)$ -frame. If we wish to  
 183 relate back to problems in which these are applied at the original line of symmetry,  $(P, M')$   
 184 (depicted in red in figure 4), we must account for the origin shift in the applied moment,  
 185 namely  $M' = M + P(t + R\alpha)$ , where  $M'$  is the moment applied at the origin in the  $(x', y')$ -  
 186 plane.

187 For small enough normal force, only the right-hand rounded part of the punch is in  
 188 contact, so that the consistency condition (3) simply gives

$$b(a) = a, \quad (32)$$

189 which is valid for  $0 < a < a_1 = \alpha R$ .

190 As the normal force increases further, the left-hand contact point moves onto the flat  
 191 part of the punch. Hence,  $b(a)$  now satisfies

$$\alpha\pi R = \sqrt{(a_1 + a)(b - a_1)} + \frac{\pi}{4}(2a_1 + a - b) + \frac{(2a_1 + a - b)}{2} \arcsin\left(\frac{2a_1 + a - b}{a + b}\right) \quad (33)$$

192 for  $a_1 < a < a_2$ , where the parameter  $a_2$  is given by the solution to the equation

$$b(a_2) = \alpha R + 2t. \quad (34)$$

193 When the applied normal force increases even further and  $a > a_2$ , the left-hand contact  
 194 edge moves onto the left-hand rounded part of the punch. Hence,  $b(a)$  then satisfies

$$\begin{aligned} \alpha\pi R = & \frac{(2a_1 + a - b)}{2} \arcsin\left(\frac{2a_1 + a - b}{a + b}\right) - \frac{(2b(a_2) + a - b)}{2} \arcsin\left(\frac{2b(a_2) + a - b}{a + b}\right) + \\ & \frac{\pi}{2}(a_1 + b(a_2) + a - b) + \sqrt{(a_1 + a)(b - a_1)} - \sqrt{(a + b(a_2))(b - b(a_2))}. \end{aligned} \quad (35)$$

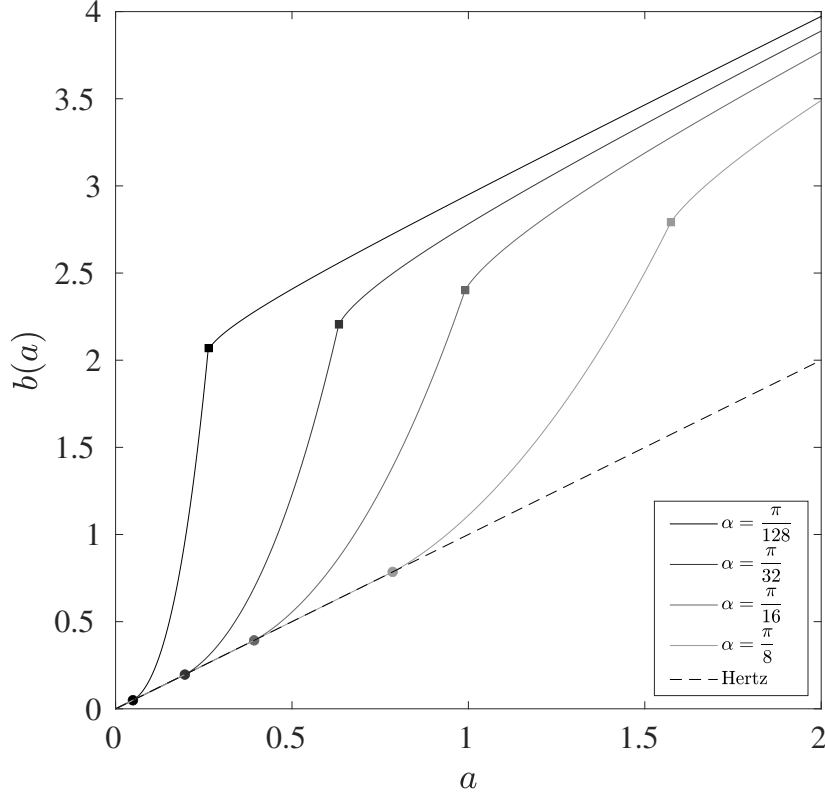


Figure 5: The left-hand contact point  $b(a)$  as a function of  $a$  for a flat-and-rounded punch at various tilt angles,  $\alpha$ . For the purposes of the plot, we have taken  $t = 1$  and  $R = 2$  and we have included the Hertzian case where  $b(a) = a$  for reference. The filled circles indicate  $a_1$ , the value of  $a$  for which  $b(a)$  moves onto the flat part of the punch and the filled squares represent  $a_2$ , where  $b(a)$  moves onto the left-hand rounded part of the punch.

195 for  $a \geq a_2$ .

196 We plot a profile of  $b(a)$  as a function of  $a$  for different tilts in figure 5. The filled  
 197 circles indicate the first transition from rounded to flat, while the filled squares indicate the  
 198 second transition from flat to the other rounded part of the punch. Note that  $b(a)$  cannot  
 199 be differentiable at  $a_1$  or  $a_2$ , so that  $K_{n,b}$  is not defined there, see (18).

200 To find the applied normal force necessary to sustain such a contact, we return to (14),  
 201 which we must invert for  $P(s)$  where  $0 < s < a$ . If  $0 < a < a_1$ , then, since  $b(a) = a$ , (14) is  
 202 a standard Abel integral equation, which is readily inverted to show that

$$P(s) = \frac{\pi\mu}{(\kappa + 1)R} s^2, \quad (36)$$

203 for  $0 < s < a$ , which is simply the solution for a Hertzian contact [11].

204 If  $a > a_1$ , since (14) must hold for all  $0 < x < a$ , it is still true that  $P(s)$  is given by (36)  
 205 for  $0 < s < a_1$ . However, for  $a_1 < x < a$  we have

$$\frac{2\pi\mu}{(\kappa + 1)R} \sqrt{x^2 - a_1^2} = \int_{a_1}^x \frac{P'(s)}{\sqrt{(x-s)(x+b(s))}} ds \text{ for } a_1 < x < a, \quad (37)$$

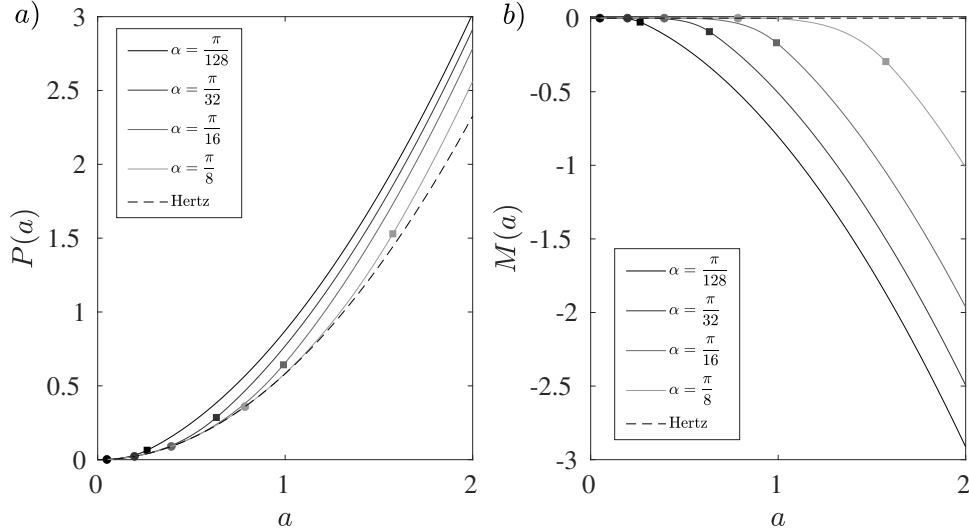


Figure 6: The (a) applied normal force and (b) applied moment necessary to sustain the contact as a function of  $a$  for a flat-and-rounded punch at various tilt angles,  $\alpha$ . For the purposes of the plot, we have taken  $t = 1$  and  $R = 2$ . The filled circles and squares perform the same function as in figure 5. For reference we have also included the equivalent curves for the Hertzian contact of a cylinder of radius  $R$ .

206 which we must invert for  $P(s)$ ,  $a_1 < s < a$ . In general, we must do this numerically.  
 207 Fortunately, this is a relatively straightforward process, which we describe in Appendix B.  
 208 We plot the resulting curve of  $P(a)$  for various tilt angles in figure 6a. Note that  $P(a)$  is  
 209 differentiable everywhere even though  $b(a)$  is not.

210 Having determined  $P(a)$ , we can utilise (16) to calculate the applied moment necessary  
 211 to maintain the tilt angle  $\alpha$  as  $P$  varies. Again, when  $0 < a < a_1$ , we can evaluate this  
 212 explicitly, finding that  $M = 0$ , as expected (as the contact is essentially Hertzian). For  
 213  $a > a_1$ , we see that

$$M(a) = \frac{1}{2} \left[ P(a)(a - b(a)) - \int_{a_1}^a P(s)(1 - b'(s)) ds \right], \quad (38)$$

214 which we can evaluate numerically using our known solutions for  $P(a)$  and  $b(a)$ . Note that  
 215 even though  $b'(s)$  is not defined when  $s = a_2$ , as it is defined everywhere else, we can still  
 216 perform the integration in (38). We plot the results in figure 6b. We note that this moment  
 217 needs to be taken in context. This is the moment about the minimum of the tilted punch  
 218 that needs to be supplied to maintain the contact. We also note that this is an illustration  
 219 of how we can sweep over values of  $\alpha$  to fill out the  $(a, \alpha)$ -space for  $M$  and  $P$ , which enables  
 220 us to ‘invert’ the problem and seek  $a$  and  $\alpha$  for a given  $(P, M)$  combination, as discussed in  
 221 §3.2; however, we will not pursue this any further in this paper.

222 Finally, we plot the  $K_n$ -coefficients (17)–(18) as functions of  $a$  for various tilt angles in  
 223 figure 7. For the left-hand coefficient, the change in behaviour  $b(a)$  as the applied normal  
 224 force increases is clear: when the left-hand contact point progresses onto the flat part of  
 225 the indenter, there is a sharp increase in  $b'(a)$ , as evidenced in figure 5. This causes  $K_{n,b}$  to  
 226 decrease until  $b(a)$  progresses to the second rounded part of the punch.

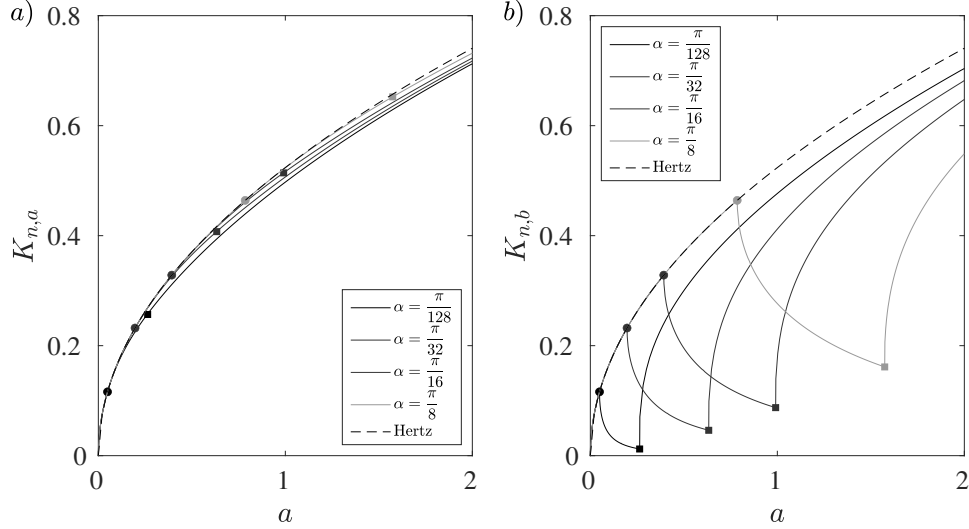


Figure 7: The (a) right-hand and (b) left-hand coefficients of the square-root expansion of the contact pressure at the contact edges as a function of  $a$  for a flat-and-rounded punch at various tilt angles,  $\alpha$ . For the purposes of the plot, we have taken  $t = 1$  and  $R = 2$ . The filled circles and squares perform the same function as in figure 5. For reference we have also included the equivalent curves for the Hertzian contact of a cylinder of radius  $R$ . The change in behaviour of  $K_{n,b}$  is due to the rapid change in  $b'(a)$  as the left-hand contact point progresses from rounded to flat (circles) and then from flat to the other round part of the punch (squares).

## 227 5. The tangential problem

228 To conclude, we briefly return to the tangential problem, that we have thus far set aside.  
 229 As discussed in section 1, for elastically-similar materials, the normal and tangential problems  
 230 decouple. Indeed, the relation between the tangential displacement gradient  $u'(x) = u'_1(x) -$   
 231  $u'_2(x)$  and the shear tractions  $q(x)$  is exactly the same as (1) with  $v$  replaced by  $u$  and  $p$   
 232 replaced by  $q$ .

233 Hence, in the case where there is purely a shear force,  $Q$ , applied in the contact (i.e. shear  
 234 tractions are not excited by differential bulk tensions), and if we assume that the normal  
 235 load is a monotonically increasing function of time and that friction is large enough for slip  
 236 to be prohibited along the whole of the contact patch, one can follow the same argument as  
 237 [11] in the non-symmetric problem to conclude that the shear traction is given by

$$q(x, a) = \begin{cases} \int_x^a \frac{G(s)}{\sqrt{(s-x)(x+b(s))}} ds & \text{for } 0 < x < a, \\ \int_{b^{-1}(-x)}^a \frac{G(s)}{\sqrt{(s-x)(x+b(s))}} ds & \text{for } -b(a) < x < 0, \\ 0 & \text{otherwise} \end{cases}, \quad (39)$$

238 where

$$Q(a) = \pi \int_0^a G(s) ds \text{ or, equivalently, } G(a) = \frac{1}{\pi} \frac{dQ}{da}. \quad (40)$$

239 When there is a differential bulk tension  $\sigma = \sigma_1 - \sigma_2$ , we must introduce a second auxiliary  
 240 function to replace (5) to find its influence on the shear traction. Extending the argument

241 of [11], we define:

$$n(x, a) = \begin{cases} \frac{x}{\sqrt{(a-x)(x+b(a))}} & \text{for } -b(a) < x < a \\ 0 & \text{otherwise} \end{cases}, \quad (41)$$

242 which, upon substituting into the tangential form of (1), induces a relative surface strain of

$$u'(x) = \frac{(\kappa + 1)}{2\mu\pi} l(x, a) \text{ where } l(x, a) = \begin{cases} \pi & \text{for } -b(a) < x < a, \\ \pi \left( 1 - \frac{|x|}{\sqrt{(a-x)(x+b(a))}} \right) & \text{otherwise} \end{cases}. \quad (42)$$

243 Then, assuming the bodies remain fully adhered in the contact region, we must find a function  
244  $H(\cdot)$  that satisfies

$$\frac{\partial}{\partial a} (\epsilon(x, a)) = \frac{\partial}{\partial a} \left( \frac{(\kappa + 1)\sigma(a)}{8\mu} + \int_0^a H(s)l(x, s) ds \right) \quad (43)$$

245 in the contact patch, where  $\epsilon(x, a)$  is the relative surface strain, [11]. Thus,

$$H(a) = -\frac{1}{4} \frac{d\sigma}{da}. \quad (44)$$

246 Therefore, in the general case, the shearing traction has a contribution from both the  
247 traction induced by the applied tangential force,  $Q$ , and a contribution from the differential  
248 bulk tension,  $\sigma$ , so that

$$q(x, a) = \begin{cases} \int_x^a \frac{G(s)}{\sqrt{(s-x)(x+b(s))}} ds + \int_x^a \frac{H(s)x}{\sqrt{(s-x)(x+b(s))}} ds & \text{for } 0 < x < a \\ \int_{b^{-1}(-x)}^a \frac{G(s)}{\sqrt{(s-x)(x+b(s))}} ds + \int_{b^{-1}(-x)}^a \frac{H(s)x}{\sqrt{(s-x)(x+b(s))}} ds & \text{for } -b(a) < x < 0, \\ 0 & \text{otherwise} \end{cases}, \quad (45)$$

249 where  $G(\cdot)$  and  $H(\cdot)$  are given by (40) and (44) respectively. We note that we can expand  
250 (45) at each end of the contact patch to find the coefficient of the square-root terms in the  
251 shear traction there, we find that

$$q(x, a) = \frac{2}{\pi} \frac{1}{\sqrt{a+b(a)}} \left( Q'(a) - \frac{\pi a \sigma'(a)}{4} \right) \sqrt{a-x} + o(\sqrt{a-x}) \text{ as } x \rightarrow a^-, \quad (46)$$

252 and

$$q(x, a) = \frac{2}{\pi b'(a)} \frac{1}{\sqrt{a+b(a)}} \left( Q'(a) + \frac{\pi b(a) \sigma'(a)}{4} \right) \sqrt{x+b(a)} + o(\sqrt{x+b(a)}) \text{ as } x \rightarrow -b(a)^+, \quad (47)$$

253 which, again, may have applications in asymptotic methods for studying partial-slip prob-  
254 lems.

## 255 6. Summary and discussion

256 In this analysis, we have demonstrated how to extend the Mossakovskii method to non-  
257 symmetric contacts in which a moment is present. The central idea is to utilise the consis-  
258 tency condition from the usual inversion of the Cauchy principal value integral relating the  
259 contact pressure and the indenter geometry as a tool to find the left-hand contact point as  
260 a function of the right (note this was arbitrarily chosen, we could have chosen to find  $a(b)$   
261 as readily as  $b(a)$ ). One can then use the Mossakovskii flat-punch superposition as in the  
262 symmetric problem to derive a non-symmetric Abel integral relating the applied normal force  
263 to the punch geometry. This is a similar idea to the use of distributions of climb dislocations  
264 as Green’s functions for the contact problem as demonstrated in [15].

265 The Abel integral formulation allows us to derive a simple relation for the necessary  
266 applied moment to sustain the contact in terms of the the contact patch size and the applied  
267 normal force, as well as straightforward expressions for the coefficients of the square-root  
268 term in the pressure expansion local to each edge of the contact, which may be of use in  
269 asymptotic methods for studying fretting fatigue in partial-slip problems [1, 9, 12].

270 We have demonstrated the methodology for two particular examples. The first example  
271 was the tilted wedge, for which analytic solutions for the applied normal force, the applied  
272 moment and the pressure coefficients can be found, and were shown to match the closed-form  
273 solutions found through an alternative route by [19]. The second, more industrially-relevant  
274 problem was that of a tilted flat-and-rounded punch. After noting that the necessity of the  
275 coordinate frame being centred at the minimum of the indenter introduced three distinct  
276 regimes in the problem, we were able to derive numerical solutions for the contact patch  
277 size, the applied normal force and the pressure coefficients, as well as the moment necessary  
278 to sustain the contact.

279 One feature of the Mossakovskii method for a general indenter when there is a moment is  
280 that one must assume that the tilt is fixed and solve the problem, which fixes the load-path  
281 in  $(P, M)$ -space that one must take to apply the method. If we do not follow this path, the  
282 minimum of the indenter changes as it rotates, which leads to issues in the formulation, as it  
283 is a history-dependent problem in the sense that it builds up the punch geometry through a  
284 series of flat punches. If one allows the indenter to rotate and the minimum to move slightly,  
285 there is part of the punch which is now not captured by the superposition of flat punches  
286 given in (7). However, since the results are load-path independent, this is only a minor point.

287 We have shown that for certain geometries such as the tilted wedge, since the minimum  
288 does not change as the normal force increases, the method can be inverted to consider the  
289 more general problem: ‘what are  $\alpha$  and  $a$  for given values of  $M$  and  $P$ ?’. Moreover, even for  
290 geometries that do not meet this condition, we can still use the given geometry found from  
291 full finite element simulations or analytic solutions as a starting point for the method, which  
292 is then able to determine the coefficients of the contact pressure at the contact edges very  
293 quickly.

294 We concluded our discussion by highlighting that, provided the contact ends both mono-  
295 tonically increasing in with the normal force and that friction is large enough to prohibit  
296 slip at all points, the methodology can readily be extended to the tangential problem in  
297 which an applied shear force and/or differential bulk tensions excite shear tractions within  
298 the contact.

299 **Appendix A. Integral expansions**

300 We shall illustrate the methodology by considering the contact pressure expansion close  
 301 to the right-hand contact point. Recall that the contact pressure for  $0 < x < a$  is given by

$$p(x, a) = \frac{1}{\pi} \int_x^a \frac{P'(s)}{\sqrt{(s-x)(x+b(s))}} ds. \quad (\text{A.1})$$

302 If  $x = a - \delta$  where  $0 < \delta \ll 1$ , we set  $s = a - \delta S$  in the integral, which yields

$$p = \frac{\sqrt{\delta}}{\pi} \int_0^1 \frac{P'(a - \delta S)}{\sqrt{(1-S)(a - \delta + b(a - \delta S))}} dS. \quad (\text{A.2})$$

303 We can then expand the integrand as  $\delta \rightarrow 0$  as a regular perturbation, which yields

$$p = \frac{\sqrt{\delta}}{\pi} \frac{P'(a)}{\sqrt{a+b(a)}} \int_0^1 \frac{1}{\sqrt{1-S}} dS + O(\delta^{3/2}), \quad (\text{A.3})$$

304 which can be evaluated and thus gives

$$K_{n,a} = \frac{2}{\pi} \frac{P'(a)}{\sqrt{a+b(a)}}. \quad (\text{A.4})$$

305 The procedure at the left-hand contact point follows a similar argument.

306 **Appendix B. Numerical solution of the non-symmetric Abel equation for the**  
 307 **flat-and-rounded punch**

308 For ease of notation, we shall set  $\mathcal{P}(s) = P'(s)$  throughout. We wish to invert the integral  
 309 equation

$$\frac{2\pi\mu}{(\kappa+1)R} \sqrt{x^2 - a_1^2} = \int_{a_1}^x \frac{P'(s)}{\sqrt{(x-s)(x+b(s))}} ds \text{ for } a_1 < x < a \quad (\text{B.1})$$

310 to find  $\mathcal{P}(s)$  for  $a_1 < s < a$ .

311 We consider a finite set of points from the range of  $a_1 < x < a$  over which the integral  
 312 equation is valid, defined by  $X_j = a_1 + j\epsilon$ , where  $\epsilon = (a - a_1)/N$  and  $j = 1, 2, \dots, N$ . We  
 313 take  $N$  to be sufficiently large so that  $0 < \epsilon \ll 1$ .

314 At the first point,  $X_1 = a_1 + \epsilon$ , the range of the integral in (B.1) is very small, so that  
 315 the integral can be asymptotically approximated to be

$$\int_{X_1-\epsilon}^{X_1} \frac{\mathcal{P}(s)}{\sqrt{(X_1-s)(X_1+b(s))}} ds = \frac{2\mathcal{P}(X_1)}{\sqrt{X_1+b(X_1)}} \sqrt{X_1 - a_1} + O(\epsilon^{3/2}). \quad (\text{B.2})$$

316 We can then simply rearrange (B.1) to find  $\mathcal{P}(X_1)$ .

317 At the next point  $X_2$ , we now know  $\mathcal{P}$  for  $0 < s < X_1$ . On that interval we can find the  
 318 interpolant of  $\mathcal{P}$ , which we shall denote  $\mathcal{P}_{int}$ . Hence, (B.1) can now be expressed as

$$\frac{2\pi\mu}{(\kappa+1)R} \sqrt{X_2^2 - a_1^2} - \int_{a_1}^{X_1} \frac{\mathcal{P}_{int}(s)}{\sqrt{(X_2-s)(X_2+b(s))}} ds = \int_{X_1}^{X_2} \frac{\mathcal{P}(s)}{\sqrt{(X_2-s)(X_2+b(s))}} ds. \quad (\text{B.3})$$

319 As before, we can then asymptotically approximate the integral on the right-hand side,  
320 finding now that

$$\int_{X_2-\epsilon}^{X_2} \frac{\mathcal{P}(s)}{\sqrt{(X_2-s)(X_2+b(s))}} ds = \frac{2\mathcal{P}(X_2)}{\sqrt{X_2+b(X_2)}} \sqrt{X_2-X_1} + O(\epsilon^{3/2}), \quad (\text{B.4})$$

321 and we then rearrange accordingly to find  $\mathcal{P}(X_2)$ .

322 This process can be iterated to find  $\mathcal{P}(a_1 + j\epsilon)$  for  $j = 1, 2, \dots, N$ , and we can integrate  
323 to find  $P(a_1 + j\epsilon)$  utilising the known boundary condition  $P(a_1) = \mu\pi a_1^2/(R(\kappa + 1))$ . We  
324 can then check convergence of the method by varying  $N$ .

## 325 References

- 326 [1] H. Andresen, D. A. Hills, J. R. Barber, and J. Vázquez. Frictional half-plane contact  
327 problems subject to alternating normal and shear loads and tension in the steady state.  
328 Intl. J. Solids Struct., 168:166–171, 2019.
- 329 [2] H. Andresen, D. A. Hills, and M. R. Moore. The steady state partial slip problem for  
330 half plane contacts subject to a constant normal load using glide dislocations. Eur. J.  
331 Mech.-A/Solids, 79:103868, 2020.
- 332 [3] H. Andresen, D. A. Hills, and J. Vázquez. Closed-form solutions for tilted three-part  
333 piecewise-quadratic half-plane contacts. Intl. J. Mech. Sci., 150:127–134, 2019.
- 334 [4] J. R. Barber. Elasticity. Springer, 2002.
- 335 [5] J. R. Barber. Contact Mechanics. Springer, 2018.
- 336 [6] M. Ciavarella. The generalized Cattaneo partial slip plane contact problem. I Theory.  
337 Intl. J. Solids Struct., 35(18):2349–2362, 1998.
- 338 [7] M. Ciavarella. The generalized Cattaneo partial slip plane contact problem. II Examples.  
339 Intl. J. Solids Struct., 35(18):2363–2378, 1998.
- 340 [8] M. Ciavarella and G. Demelio. On non-symmetrical plane contacts. Intl. J. Mech. Sci.,  
341 41:1533–1550, 1999.
- 342 [9] R. M. N. Fleury, D. A. Hills, R. Ramesh, and J. R. Barber. Incomplete contacts in  
343 partial slip subject to varying normal and shear loading, and their representation by  
344 asymptotes. J. Mech. Phys. Solids, 99:178–191, 2017.
- 345 [10] F. D. Gakhov. Boundary Value Problems. Pergamon, 1966.
- 346 [11] D. A. Hills, M. Davies, and J. R. Barber. An incremental formulation for half-plane  
347 contact problems subject to varying normal load, shear, and tension. J. Strain Anal.  
348 Eng. Des., 46(6):436–443, 2011.
- 349 [12] D. A. Hills, R. M. N. Fleury, and D. Dini. Partial slip incomplete contacts under  
350 constant normal load and subject to periodic loading. Intl. J. Mech. Sci., 108:115–121,  
351 2016.



- 352 [13] D. A. Hills, R. Ramesh, J. R. Barber, and M. R. Moore. Methods to solve half-plane  
353 partial slip contact problems. International Journal of Solids and Structures, 155:155–  
354 159, 2018.
- 355 [14] J. Jäger. A new principle in contact mechanics. ASME J. Tribol., 120:677–684, 1998.
- 356 [15] M. R. Moore and D. A. Hills. Solution of half-plane contact problems by distributing  
357 climb dislocations. Intl. J. Solids Struct., 2018.
- 358 [16] M. R. Moore, R. Ramesh, D. A. Hills, and J. R. Barber. Half-plane partial slip contact  
359 problems with a constant normal load subject to a shear force and differential bulk  
360 tension. J. Mech. Phys. Solids, 118:245–253, 2018.
- 361 [17] V. I. Mossakovskii. Application of the reciprocity theorem to the determination of the  
362 resultant forces and moments in three-dimensional contact problems. PMM, 17:477–482,  
363 1953.
- 364 [18] R. Ramesh, J. R. Barber, and D. A. Hills. Plane incomplete contact problems subject  
365 to bulk stress with a varying normal load. Intl. J. Mech. Sci., 122:228–234, 2017.
- 366 [19] A. Sackfield, D. Dini, and D. A. Hills. The tilted shallow wedge problem. Eur. J.  
367 Mech.-A/Solids, 24(6):919–928, 2005.
- 368 [20] D. A. Spence. An eigenvalue problem for elastic contact with finite friction. In Math.  
369 Proc. Camb. Phil. Soc., volume 73, pages 249–268, 1973.